Central European Journal of Energetic Materials
ISSN 1733-7178; e-ISSN 2353-1843

Cent. Eur. J. Energ. Mater. 2024, *21*(1): 5-21; DOI 10.22211/cejem/184038
Article is available in PDF-format, in colour, at:
https://ipo.lukasiewicz.gov.pl/wydawnictwa/cejem-woluminy/vol-21-nr-1/

Research paper

Synthesis of a New Random Copolymer Based on Glycidyl Nitrate and Tetrahydrofuran: A Thermal, Kinetic, and Theoretical Study

Milad Alizadeh, Yadollah Bayat*)
Department of Chemistry and Chemical Engineering, Malek Ashtar University of Technology, Tehran, Iran
* *E-mail:* y_bayat@mut.ac.ir

Abstract: Today, polymeric binders are regarded as playing a crucial role in solid propellants. Therefore, research aimed at improving the performance of the binder is particularly important. In this study, a new energetic random copolymer of glycidyl nitrate (GN) and tetrahydrofuran (THF), poly (THF-ran-GN) (M_n = 1561 g mol^{-1}) was synthesized using the cationic ring-opening polymerization process. The chemical structure of the prepared copolymers was characterized utilizing FT-IR, ^{1}H NMR and ^{13}C NMR spectroscopic techniques. The thermal properties of the copolymers and their molecular weights were investigated by thermogravimetric analysis (TGA), differential thermal analysis (DTA), differential scanning calorimetry (DSC) and gel permeation chromatography (GPC). The results showed that the glass transition temperatures (T_g) of the synthesized copolymers (T_g= −59 °C) were lower than those of pure PGN (T_g= −32 °C). Therefore, copolymerization led to a decrease in the T_g temperature. The kinetic parameters of the DSC were determined in the non-isothermal framework described by Kissinger. The electronic structure of the copolymers was also simulated with the Gaussian 09 program package in order to investigate the optoelectronic properties of the copolymers based on time dependent density functional theory (TD-DFT) computations. In addition, the existence of three peaks featuring significant excitations associated with electron transition in frontier orbitals was demonstrated. The results showed that the new synthesized random copolymer has energetic properties.

Keywords: glycidyl nitrate copolymers, thermal properties, kinetic study, optoelectronic properties, binder, ring opening polymerization

Supplementary Information (SI):

SI contains FT-IR, ^{1}H NMR, ^{13}C NMR spectra and electronic excitations in the frontier molecular orbitals and the original DSC thermograms depicted in Figure 8.

1 Introduction

In the propellant literature, the relative importance of binders has been subject to considerable debate [1-31]. In simpler terms, binders as polymeric systems have an influence on the preservation and fixing of propellant elements, as well as their formulation and mechanical properties [1-6, 9]. Two main classifications of binders are neutral and energetic, such as [7, 8]:

– polybutadiene acrylic acid-acrylonitrile (PBAN),
– polypropylene glycol (PPG),
– polyethylene glycol (PEG),
– polycaprolactone (PCL),
– hydroxyl-terminated polybutadiene (HTPB), and
– nitrated hydroxyl-terminated polybutadiene (NHTPB),
– polyglycidyl nitrate (PGN),
– glycidyl azide polymer (GAP),

respectively. In fact, neutral binders possess suitable properties such as loading volume of solids, low T_g, good flexibility and high tensile strength [10-12]. While neutral binders with these properties are generally employed, they do not possess suitable energetic properties [13]. In order to address these defects, neutral binders can be used in conjuction with the second type of binders. This is because the latter have the ability to increase the burning rate and impulse of solid propellants, give excellent explosive fire, a suitable density, and a great fire blast [14-18].

Modifying an energetic binder with a neutral binder is a standard method for producing a new binder with the desired properties. An example of an active and energetic binder is PGN, which is often used in solid propellant formulations [19]. This binder can be converted into a copolymer binder by combining it with the PCL, polytetrahydrofuran (PTHF), propylene oxide (PO), and some other polyethers [20-25]. The synthesis of PGN-based copolymers can produce a new class of polymer with good mechanical and energetic properties [26].

In the present work, a random copolymer was synthesized using THF and GN to improve the properties of the PGN binder. The synthesis of this unique random copolymer involves a ring-opening polymerizations. The presence of the

THF reduces the T_g and improves the flexibility compared to the PGN binder. Furthermore, the thermal and kinetic properties, such as thermal (exothermic) decomposition, thermal stability, and activation energies of the energetic materials were analyzed. The Kissinger and Flynn-Wall-Ozawa (FWO) methods were used in order to determine the kinetic parameters under a non-isothermal state [28, 29]. The standard methods used were TGA, DTA and DSC [27]. Finally, the optoelectronic properties of the synthesized copolymer were investigated [30, 31].

2 Experimental

2.1 Materials and methods

Boron trifluoride etherate ($BF_3 \cdot OEt_2$), dichloromethane (DCM), sodium hydroxide (NaOH), 1,4-butanediol (BDO), sodium bicarbonate ($NaHCO_3$), potassium nitrate (KNO_3), sodium sulfate (Na_2SO_4), nitric acid (HNO_3, 60%), epichlorohydrin (ECH), and tetrahydrofuran (THF) were purchased from Merck company. Infrared spectra were conducted using a Mbb Bomem Mb-100 FT-IR spectrometer, which is based on Fourier transform infrared (FT-IR) analysis. ^{1}H NMR spectra were obtained using a 400 MHz Bruker spectrometer, with tetramethylsilane (TMS) as the internal standard and deuterated chloroform ($CDCl_3$) as the solvent for product dissolution. The thermal properties of the new copolymers were recorded using a NETZSCH 200F3 (Germany) model, with a nitrogen purge and a speed of 10 °C min^{-1}. Gel permeation chromatography (GPC) was performed using an Agilent 1100 system, with THF and polystyrene (PS) as solvent and standard.

2.2 Synthesis of glycidyl nitrate (GN)

A 100 mL two-necked round-bottomed flask equipped with a magnetic stirrer bar was utilized. The flask was fitted to a dropping funnel and a condenser. Solid KNO_3 (12.12 g, 0.12 mol) and 60% HNO_3 (20 mL) solution were added to the flask. The reaction temperature was maintained at 10 °C. ECH (37 g, 2 mol) was added by a dropping funnel during 3 h with slow stirring. After the addition of the ECH was complete, the temperature was kept for 3 h in the range of 9-14 °C. Subsequently, a 50% aqueous solution of NaOH (44.8 g) was added to the mixture at 7 °C during 3 h. After the addition of the NaOH, the mixture was kept stirring during 24 h. The organic layer was extracted with DCM (3×20 mL), and the combined organic layers were subsequently washed with water (3×40 mL). The organic layer was then dried over Na_2SO_4 (10 g), and the solvent was evaporated under vacuum conditions. Due to the energetic nature of

the final products, it can be distillated at 10 mmHg and 45 °C. The yield obtained was 28.8 g, corresponding to a percentage yield of 62%.

2.3 Synthesis of a new random copolymer of tetrahydrofuran-glycidyl nitrate, poly (THF-ran-GN)

In a nitrogen atmosphere, a 100 mL round-bottomed flask equipped with a magnetic stirrer bar was fitted with a dropping funnel. The flask was charged with dry DCM (10 mL) as the solvent, and BDO (0.56 g, 0.013 mol) dried with 4 Å molecular sieves was added as the polymerization initiator. Afterwards, $BF_3{\cdot}OEt_2$ (0.5 mL, 0.004 mol) was introduced as the catalyst, still under a nitrogen atmosphere. The temperature was maintained at 5 °C and slowly stirred for 10 min. During the mixing process, a mixture of GN (10.5 g, 0.088 mol) and THF (6.52 g, 0.090 mol) in of dry DCM (10 mL) was added dropwise over a period of 50 min. Stirring was continued at 5-10 °C for 48 h. A light-yellow coloured solution was obtained, and the reaction was then quenched using water (5 mL). The final product was extracted using dry DCM (50 mL). The copolymer solution was washed with aqueous $NaHCO_3$ (25 wt.%), dried with magnesium sulfate ($MgSO_4$), and the DCM was evaporated under vacuum conditions. This process yielded the copolymer poly (THF-ran-GN). The yield was 15.7 g (80%), with a number average molecular weight (M_n) of 1561 g mol^{-1}:

- **GPC analysis**: M_W = 2411 g mol^{-1}, M_n = 1561 g mol^{-1}, PDI = 1.455,
- **^{1}H NMR** (400 MHz, $CDCl_3$) δ [ppm]: 1.10 (–C**H**$_2$–CH_2O), 3.2-4 (C**H**$_2$O) and (C**H**O), 4.4-4.60 (–C**H**$_2$$ONO_2$),
- **^{13}C NMR**, (100 MHZ $CDCl_3$) δ [ppm]: 26 (**C**H_2CH_2O), 72.85 (–**C**H_2O), 73.83 (–**C**H_2ONO_2), 75.18 (**C**HO),
- **FT-IR** (KBr) [cm^{-1}]: 3428, 2868, 1634, 1279, 1118 and 857.

2.4 E_a calculation during thermal decomposition

Various methods are employed in order to investigate thermal decomposition, the TGA method being particularly practical. Additionally, the Kissinger method is used as given in Equation 1 [32-34].

$$\ln(\beta/T_m^2) = -E_a/RT_m \quad (1)$$

where β, T_m, E_a and R are the different heating rates, the maximum temperature of weight loss, activation energy, and universal gas constant, respectively. The graph slope of $\ln(\beta/T_m^2)$ is correlated with the measured T_m. According to Equation 1, the slope of the plot of $\ln(\beta/T_m^2)$ against $)1/T_m)$ is equivalent to $(-E_a/R)$. Consequently, the E_a value can be determined from the slope [35].

Other methods used to calculate the E_a of decomposition include the FWO method in the following form [36-38]:

$$\log \beta = C - (0.4567E_a/RT_a) \quad (2)$$

where the E_a can be determined by analyzing the slope of the log β against $1/T_a$.

2.5 Computational details

The geometric and electronic structure of the copolymer was investigated using density functional theory (DFT) methods in order to gain insight into its optoelectronic properties. The local minimum geometry of this copolymer was obtained with hybrid DFT exchange-correlation functional and an all-electron basis sets, such as B3LYP and 6-31g(d), after a DFT calibration method using Gaussian 09 program package [38-43]. Taking into account the ground state structure of the copolymer unit cell, its electronic absorption spectra was calculated with TD-DFT [44].

3 Measurement and Results

3.1 Synthesis of the new copolymer poly (THF-ran-GN)

A new random copolymer, namely poly (THF-ran-GN) (M_n = 1561 g mol^{-1}) was synthesized using $BF_3 \cdot OEt_2$ as a catalyst for cationic ring-opening of GN and THF. The copolymerization reaction was initiated with BDO (Figure 1).

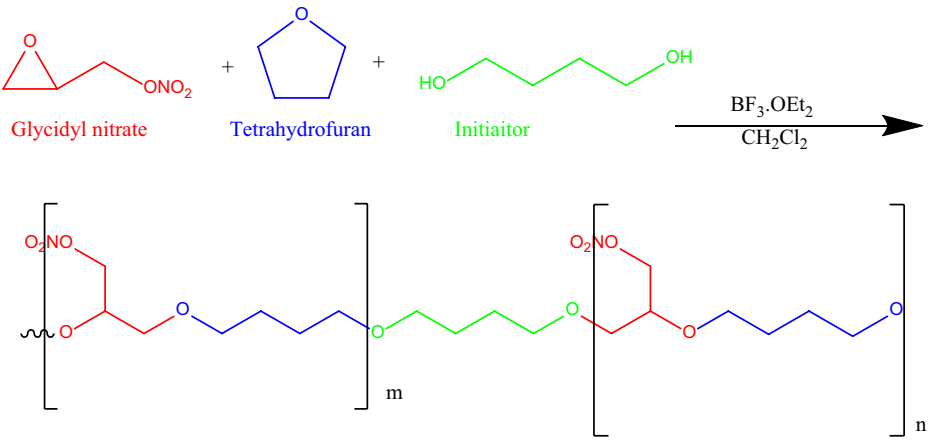

Figure 1. Copolymerization reaction in the synthesis of poly (THF-ran-GN)

3.2 Verification of poly (THF-ran-GN) copolymer

The structure of random copolymer poly (THF-ran-GN) was characterized using spectroscopy. The FT-IR spectra of poly (THF-ran-GN) and PGN are presented in the first Supplementary Information (SI, Figure S1). The structure of the synthesized copolymer was also characterized using nuclear magnetic resonance (NMR) spectroscopy, as shown in SI, Figures S2 and S3.

The poly (THF-ran-GN) FTIR spectrum displays peaks at 3428, 2868, 1634, 1279, 1118, and 857 cm^{-1}, which correspond to the PTHF and PGN fragments. These peaks represent the vibration of –OH, $–CH_2$, symmetrical and unsymmetrical vibration of $–NO_2$, C–O groups and stretching of N–O, respectively. These peaks confirm the presence of the copolymer structure of poly (THF-ran-GN).

In the NMR spectra (Figure S2), the signal observed at 1.55 ppm was assigned to the methylene of the opened THF ring and the catalyst methylene protons. Multiple peaks ranging from 3.2 to 4 ppm indicated the presence of methylene protons of $–CH_2O$, while the methylene protons of $–CH_2ONO_2$ units were observed at 4.4-4.60 ppm. The ^{1}H NMR spectrum indicated that the peak at 1.2 ppm corresponded to the ($O–CH_2–CH_3$) group of the catalyst and the opened THF ring [45, 46]. Additionally, ^{1}H NMR spectroscopy was used to ascertain the molar percentages of the two monomers used in the copolymerization process [47]. These results indicated that GN exhibits greater reactivity compared to THF in this copolymerization, with 66.36 mol% GN and 33.64 mol% THF, respectively. ^{13}C NMR analysis (see Figure S3), of poly (THF-ran-GN) exhibited distinct peaks at 26.3 ($\mathbf{C}H_2CH_2O$), 72.85 ($–\mathbf{C}H_2O$), 73.83 ($–\mathbf{C}H_2ONO_2$) and 75.18 (**C**H–O), which correspond to the structure of the newly synthesized copolymer [48, 49].

GPC analysis of the synthesized poly (THF-ran-GN) is shown in Figure 2, and revealed values of M_w, M_n, and PDI for the copolymer as 1561 and 2411 g mol^{-1}, and 1.455, respectively.

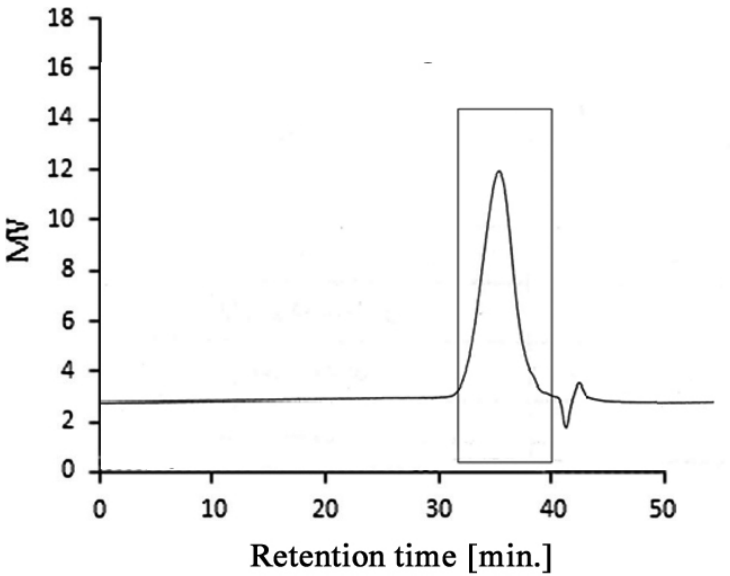

Figure 2. GPC plot of poly (THF-ran-GN)

3.3 Thermal properties of poly (THF-ran-GN) copolymer

The DSC thermogram (see Figure 3) displays the thermal properties of the copolymer poly (THF-ran-GN). The results for the random copolymer indicated the occurence of a single point for the T_g, which is influenced by the purity of THF and GN utilized in the copolymerization process. The T_g value of the new copolymer is lower (T_g = –59 °C) than that of PGN (T_g = –32 °C), which can be attributed to the presence of the flexible units in PTHF (T_g = –85 °C). This outcome suggests that the copolymerization reaction has improved the T_g value of the copolymer.

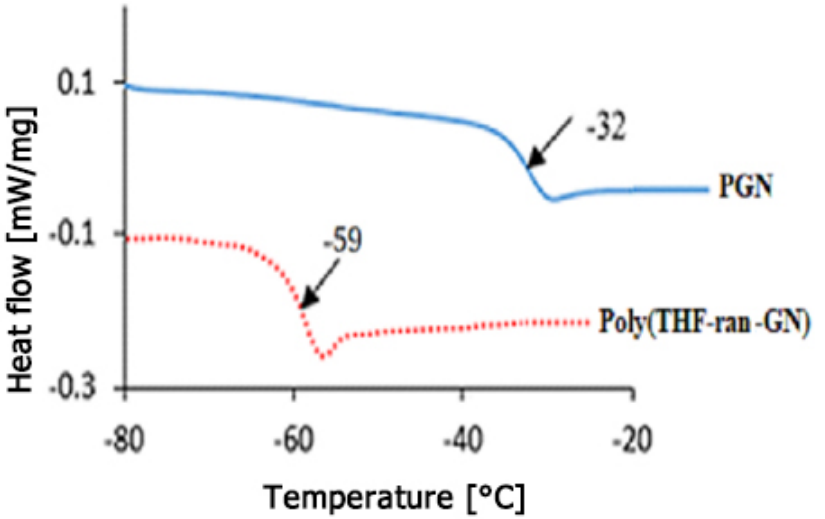

Figure 3. DSC thermogram of PGN and poly (THF-ran-GN)

3.4 Theoretical results

The low lying unit cell structure of the open shell copolymer was obtained without any symmetry constraints (C1 symmetry), see Figure 4. No imaginary frequency in this structure confirms the local minimization of its geometry. The frontier molecular orbitals in the TD-DFT framework and optoelectronic properties were studied using the UV spectrum. A few peaks are visible in the areas 295-335, 435-565, and 3235 nm, with verifiable oscillator strength. The existence of peaks in Figure 5 confirms the highly energetic properties of the copolymer. These peaks are related to electrons in the frontier orbitals with high excitation. The developed form of these peaks can be seen in Figure 6. In SI (Figure S4), a lot of electron movements in the molecular orbitals of the investigated copolymer are visible. It is known that α- and β-electron transitions increase oscillation strengths.

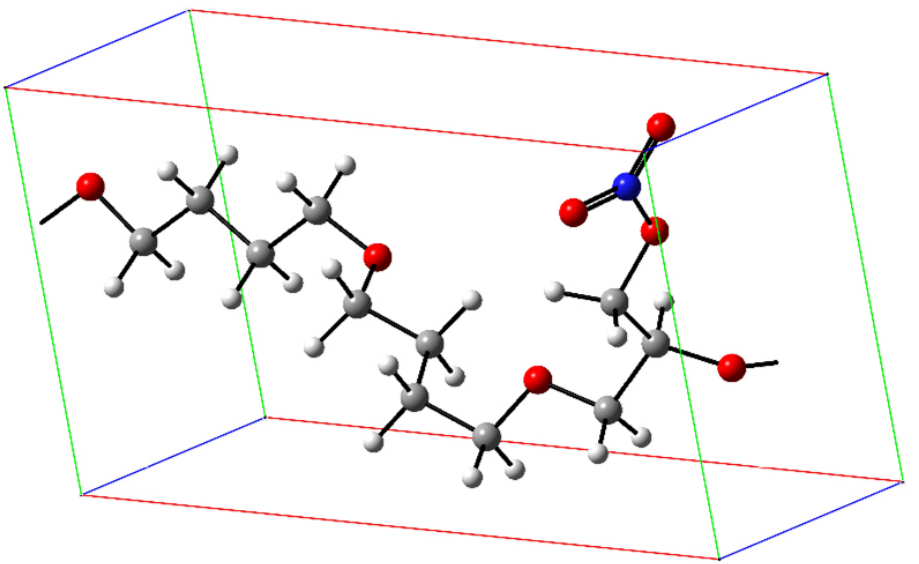

Figure 4. Optimized unit cell structure of copolymer at B3LYP/6-31G (d) level of theory

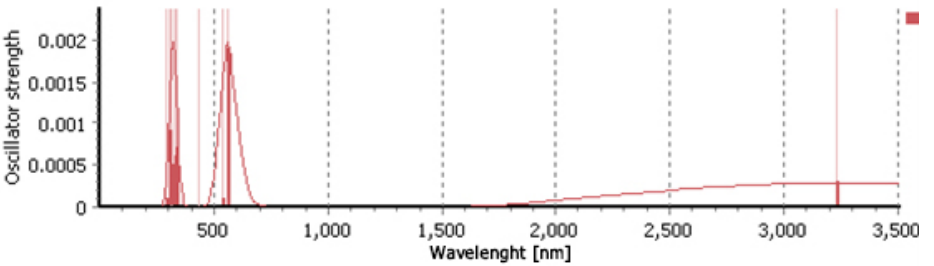

Figure 5. Calculated UV spectrum of the copolymer at the selected level of theory

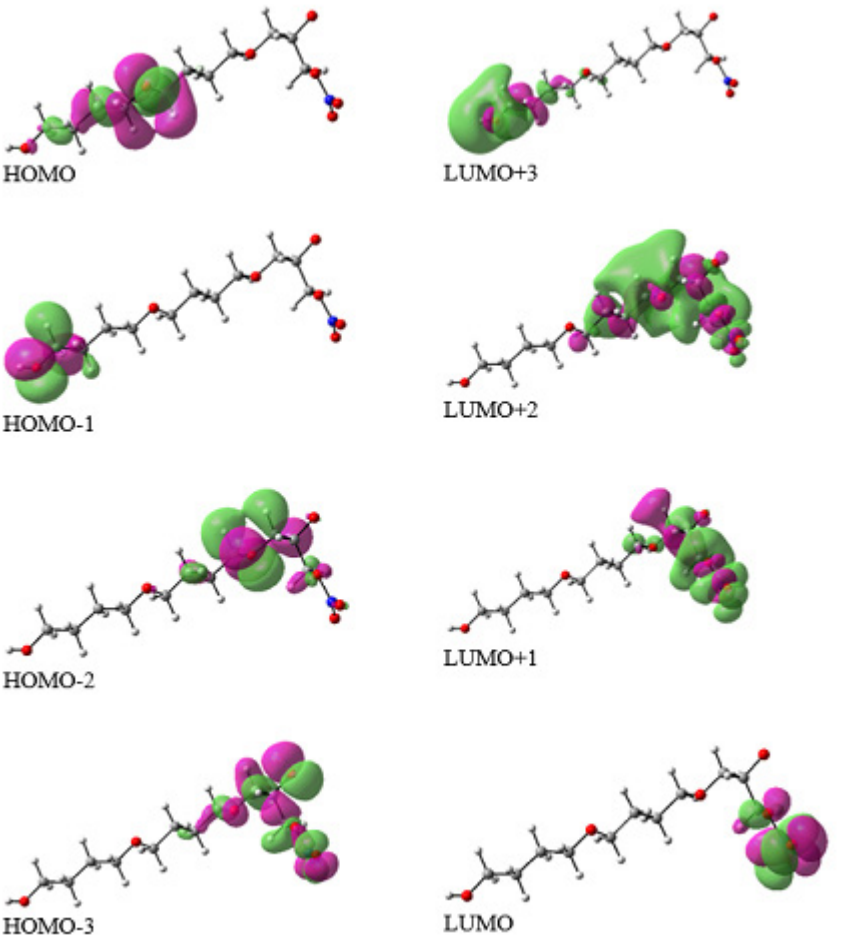

Figure 6. Frontier molecular orbitals of the copolymer

3.5 Thermal decomposition of the synthesized poly (THF-ran-GN)

Various heating rates were utilized to study the decomposition of the copolymer. The copolymer's DSC analysis was conducted at rates of 5, 10, 15, 20 K·min^{-1}, ranging from 25 to 400 °C. As the heating rate was increased, the decomposition temperature was observed to shift towards higher temperatures. Figures 7 and 8 illustrate the relationship between heating rate and temperature, indicating that the decomposition enthalpy (ΔH) increased with heating rate. An exothermic decomposition (Figures 7 and 8 (see SI, Figures S5-S8) occurs at 204.87, 212.66, 221.46, and 224.57 °C at heating rates of 5, 10, 15, and 20 K·min^{-1}, respectively.

The DSC curves show a reliable effect on the decomposition process of the random copolymer (Figure 8). According to the DSC analysis, there is a single peak for the synthesized copolymer; increasing the heating rate mainly leads to an increase in the decomposition temperature (DT) (in °C) and ΔH (in $J \cdot g^{-1}$). Comparing the ΔH values of PGN ($-348\ J \cdot g^{-1}$) [1] with those of this copolymer at heating rates of 5 and 10 $K \cdot min^{-1}$, it may be concluded that the decomposition energy is decreased in the random copolymer at these heating rates. So, creating the copolymer from PGN causes a decrease in the ΔH. There are inverse trends at 15 and 20 $K \cdot min^{-1}$ heating rates for the ΔH values.

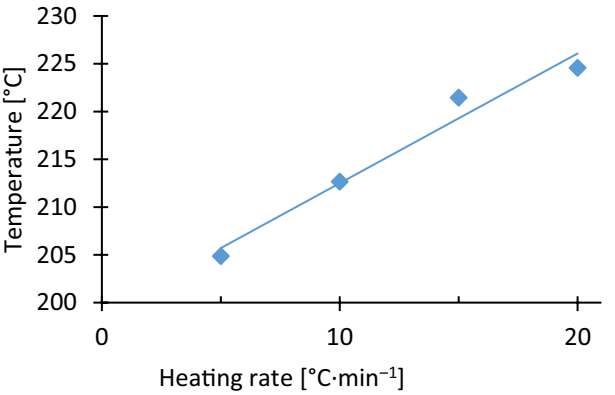

Figure 7. Heating rate versus temperature in the range of 200 to 230 °C

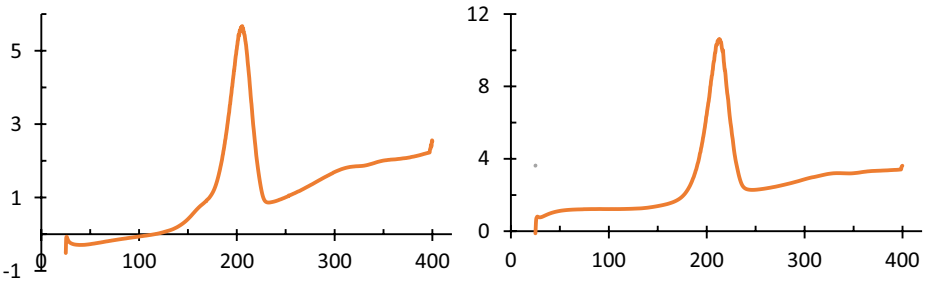

(a) ($-156.65\ J\ g^{-1}$) (b) ($-310.11\ J\ g^{-1}$)

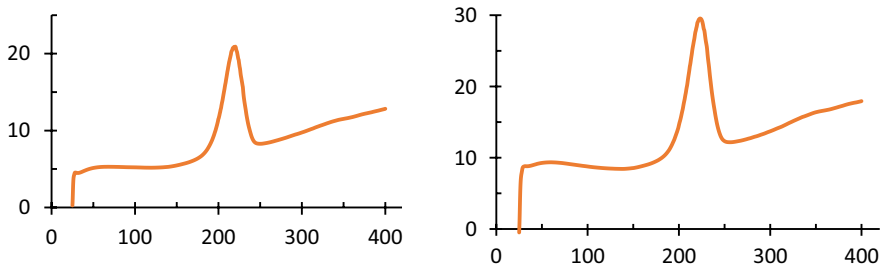

(c) (–286.85 J g^{-1}) (d) (–1184.11 J g^{-1})

Figure 8. DSC thermograms and ΔH values for the copolymer in the range of 25 to 400 °C at heating rates of 5 (a), 10 (b), 15 (c), and 20 (d) K min^{-1} (see original thermograms in SI, Figures S5-S8)

3.6 Kinetic study of the thermal decomposition

In the Kissinger method, the regression (R^2) analysis gave a value of 0.97, indicating the copolymer's linear behaviour. According to its equation line, $y = -13.74x + 19.77$, the E_a value for decomposition was 114 kJ·mol^{-1}, as in other reports, 117 kJ·mol^{-1} [20]. Furthermore, the degradation rate (K) and half-life of decomposition ($T_{1/2}$) of the synthesized copolymer are predicted using Equations 3 and 4.

$$K = A \exp^{-Ea/RT} \tag{3}$$

where A, R, and T are the pre-exponential factor, universal gas constant, and absolute temperature, respectively.

$$T_{1/2} = 0.658/K \tag{4}$$

Based on Equation 3 and the E_a value, at 50 °C the copolymer exhibits $T_{1/2}$ value of 5.6 y.

4 Conclusions

- The synthesis of random copolymer poly (THF-ran-GN) was confirmed using spectroscopic techniques. A cationic ring-opening reaction was utilized for opening the cationic rings of glycidyl nitrate (GN) and tetrahydrofuran (THF) to produce poly (THF-ran-GN) (M_n = 1561 g mol^{-1}). The new

copolymer consists of 66.36 mol% GN, and 33.64 mol% THF.

- The results show that the T_g of this copolymer is –59 °C, which falls between the T_g values of PGN (–32 °C) and PTHF (–85 °C).
- In terms of the kinetic study, the E_a and half-life at 50 °C are 114 kJ mol^{-1} and 5.6 y, respectively.
- Theoretical analysis of the synthetic copolymer reveals that its energetic properties are associated with the nitro ester structure. Numerous oscillator electrons confirm the energetic nature of structures derived from nitrate esters. Moreover, significant excitations with high oscillation strengths suggest a highly energetic potential for this copolymer.

References

[1] Ashish, J.; Swaroop, G.; Balasubramanian, K. Effect of Ammonium Perchlorate Particle Size on Flow, Ballistic, and Mechanical Properties of Composite Propellant. In: *Nanomaterials in Rocket Propulsion Systems.* (Yan, Q.; He, G.; Liu, P.; Gozin, M.; Eds.) Elsevier Inc., Chapter 8, pp. 299-362, **2019**; ISBN 978-0-12-813908-0.

[2] Babuk, V.A.; Vassiliev, V.A.; Sviridov, V.V. Propellant Formulation Factors and Metal Agglomeration in Combustion of Aluminized Solid Rocket Propellant. *Combust. Sci. Technol.* **2001**, *163*(1): 261-289; https://doi.org/10.1080/00102200108952159.

[3] Oommen, C.; Jain, S.R. Ammonium Nitrate: A Promising Rocket Propellant Oxidizer. *J. Hazard. Mater.* **1999**, *67*(3): 253-81; https://doi.org/10.1016/S0304-3894(99)00039-4.

[4] Chaturvedi, S.; Dave, P.N. Solid Propellants: AP/HTPB Composite Propellants. *Arabian J. Chem.* **2019**, *12*(8): 2061-2068; https://doi.org/10.1016/j.arabjc.2014.12.033.

[5] Cohen, N.S.; Fleming, R.W.; Derr, R.L. Role of Binders in Solid Propellant Combustion. *AIAA J.* **1974**, *12*(2): 212-218; https://doi.org/10.2514/3.49195.

[6] Yadav, N.; Srivastava, P.K.; Varma, M. Recent Advances in Catalytic Combustion of AP-based Composite Solid Propellants. *Def. Technol.* **2021**, *17*(3): 1013-1031; https://doi.org/10.1016/j.dt.2020.06.007.

[7] Ghoroghchian, F.; Bayat, Y.; Abrishami, F. Study on the Thermal Stability and Decomposition Kinetics of Polypropylene Glycol–Glycidyl Azide Polymer–Polypropylene Glycol (PPG-GAP-PPG) as a Novel Triblock Copolymer Binder. *Cent. Eur. J. Energ. Mater.* **2020**, *17*(2): 251-289; http://dx.doi.org/10.22211/cejem/124073.

[8] Schock, M.; Bräse, S. Reactive & Efficient: Organic Azides as Cross-linkers in Material Sciences. *Molecules* **2020**, *25*(4): paper 1009; https://doi.org/10.3390/molecules25041009.

[9] Khanlari, T.; Bayat, Y.; Bayat, M. Synthesis, Thermal Stability and Kinetic Decomposition of Triblock Copolymer Polypropylene Glycol – poly Glycidyl

Nitrate – Polypropylene Glycol (PPG–PGN–PPG). *Polym. Bull.* **2020**, *77*: 5859-5878; https://doi.org/10.1007/s00289-019-03051-z.

[10] O'Sullivan, O.T.; Zdilla, M.J. Properties and Promise of Catenated Nitrogen Systems as High-Energy-Density Materials. *Chem. Rev.* **2020**, *120*(12): 5682-5744. https://doi.org/10.1021/acs.chemrev.9b00804.

[11] Zhou, S.; Tang, G.; Pang, A.; Guo, X.; Wu, F.; Song, H.; Xu, X.; Hu, X.; Wang, Y. Synthesis of an Alkynyl Neutral Polymer-bonding Agent and Its Enhancing Effect on Tensile Strength of Glycidyl Azide Polymer-based Propellants. *Iran. Polym. J.* **2019**, *28*(11): 943-955; https://doi.org/10.1007/s13726-019-00756-w.

[12] Nayak, R.; Padhye, R.; Sinnappoo, K.; Arnold, L.; Behera, B.K. Airbags. *Text. Prog.* **2013**, *45*(4): 209-301; https://doi.org/10.1080/00405167.2013.859435.

[13] Sun Min, B. Characterization of the Plasticized GAP/PEG and GAP/PCL Block Copolyurethane Binder Matrices and Its Propellants. *Propellants Explos. Pyrotech.* **2008**, *33*(2): 131-138; https://doi.org/10.1002/prep.200700241.

[14] Yuan, H.; Huang, J.Q.; Peng, H.J.; Titirici, M.M.; Xiang, R.; Chen, R.; Liu, Q.; Zhang, Q. A Review of Functional Binders in Lithium–Sulfur Batteries. *Adv. Energy Mater.* **2018**, *8*(31): paper 1802107; https://doi.org/10.1002/aenm.201802107.

[15] Cheng, T. Review of Novel Energetic Polymers and Binders–high Energy Propellant Ingredients for the New Space Race. *Des. Monomers Polym.* **2019**, *22*(1): 54-65. https://doi.org/10.1080/15685551.2019.1575652.

[16] Mohan, Y.M.; Mani, Y.; Raju, K.M. Synthesis of Azido Polymers as Potential Energetic Propellant Binders. *Des. Monomers Polym.* **2006**, *9*(3): 201-236; https://doi.org/10.1163/156855506777351045.

[17] Badgujar, D.M.; Talawar, M.B.; Zarko, V.E.; Mahulikar, P.P. New Directions in the Area of Modern Energetic Polymers: An Overview. *Combust. Explos. Shock Waves* **2017**, *53*: 371-387. https://doi.org/10.1134/S0010508217040013.

[18] Shee, S.K.; Reddy, S.T.; Athar, J.; Sikder, A.K.; Talawar, M.B.; Banerjee, S.; Khan, M.A. Probing the Compatibility of Energetic Binder poly-Glycidyl Nitrate with Energetic Plasticizers: Thermal, Rheological and DFT Studies. *RSC Adv.* **2015**, *5*(123): 101297-101308. https://doi.org/10.1039/C5RA16476A.

[19] Talawar, M.B.; Sivabalan, R.; Mukundan, T.; Muthurajan, H.; Sikder, A.K.; Gandhe, B.R.; Rao, A.S. Environmentally Compatible Next Generation Green Energetic Materials (GEMs). *J. Hazard. Mater.* **2009**, *161*(2-3): 589-607; https://doi.org/10.1016/j.jhazmat.2008.04.011.

[20] Abrishami, F.; Zohari, N.; Zeynali, V. Synthesis and Kinetic Study on the Thermal Degradation of Triblock Copolymer of Polycaprolactone – poly (Glycidyl Nitrate) – Polycaprolactone (PCL-PGN-PCL) as an Energetic Binder. *Polym. Adv. Technol.* **2019**, *30*(3): 640-647; https://doi.org/10.1002/pat.4500.

[21] Khanlari, T.; Bayat, Y.; Bayat, M.; Sheibani, N. Synthesis, Characterization, and Curing of Propylene Oxide and Glycidyl Nitrate Random Copolymer (GN-ran-PO) and Investigation of Its Compatibility with Different Energetic Plasticizers. *J. Mol. Struct.* **2021**, *1231*: paper 130008; https://doi.org/10.1016/j.molstruc.2021.130008.

[22] Ghorbani, M.; Bayat, Y.; Mossahebi Mohammadi, M.; Jafari, S. Synthesis and

Characterization of PGN–PTHF–PGN as a New Triblock Copolymer. *Proc. 11th Int. Sem. on Polymer Science and Technology,* **2014**; https://www. civilica. com/Paper-ISPST11-ISPST11_272.html.

[23] Khanlari, T.; Bayat, Y.; Bayat, M. Optimization of Factors Affecting the Synthesis of Polypropylene Glycol/Polyglycidyl Nitrate/Polypropylene Glycol Triblock Copolymer and Evaluation of Its Thermal Properties. (in Persian) *Iran. J. Polym. Sci. Technol.* **2020**, *33*(1): 63-73.

[24] Peng, W.; Ranganathan, R.; Keblinski, P.; Akcora, P.; Ozisik, R. Viscoelastic and Dynamic Properties of Polymer Grafted Nanocomposites with High Glass Transition Temperature Graft Chains. *J. Appl. Phys*. **2019**, *126*(19): paper 195102; https://doi.org/10.1063/1.5119694.

[25] Kim, B.; Chae, C.G.; Satoh, Y.; Isono, T.; Ahn, M.K.; Min, C.M.; Hong, J.H.; Ramirez, C.F.; Satoh, T.; Lee, J.S. Synthesis of Hard–Soft–Hard Triblock Copolymers, Poly (2-Naphthyl Glycidyl Ether)-block-poly [2-(2-(2-Methoxyethoxy) Ethoxy) Ethyl Glycidyl Ether]-block-poly (2-Naphthyl Glycidyl Ether), for Solid Electrolytes. *Macromol.* **2018**, *51*(6): 2293-2301; https://doi.org/10.1021/acs.macromol.7b02553.

[26] Kohga, M.; Okamoto, K. Thermal Decomposition Behaviors and Burning Characteristics of Ammonium Nitrate/Polytetrahydrofuran/Glycerin Composite Propellant. *Combust. Flame* **2011**, *158*(3): 573-582; https://doi.org/10.1016/j.combustflame.2010.10.009.

[27] Wang, Q.; Wang, L.; Zhang, X.; Mi, Z. Thermal Stability and Kinetic of Decomposition of Nitrated HTPB. *J. Hazard. Mater.* **2009**, *172*(2-3): 1659-1664; https://doi.org/10.1016/j.jhazmat.2009.08.040.

[28] Hassan, M.A.; Shehata, A.B. Studies on Some Acrylamido Polymers and Copolymer as Stabilizers for Nitrocellulose. *J. Appl. Polym. Sci.* **2002**, *85*(14): 2808-2819; https://doi.org/10.1002/app.10834.

[29] Martin, J.L.; Cadenato, A.; Salla, J.M. Comparative Studies on the non-Isothermal DSC Curing Kinetics of an Unsaturated Polyester Resin Using Free Radicals and Empirical Models. *Thermochim. Acta* **1997**, *306*(1-2): 115-126; https://doi.org/10.1016/S0040-6031(97)00311-0.

[30] Coleone, A.P.; Lascane, L.G.; Batagin-Neto, A. Polypyrrole Derivatives for Optoelectronic Applications: A DFT Study on the Influence of Side Groups. *Phys. Chem. Chem. Phys.* **2019**, *21*(32): 17729-17739; https://doi.org/10.1039/C9CP02638J.

[31] Botiz, I.; Stingelin, N. Influence of Molecular Conformations and Microstructure on the Optoelectronic Properties of Conjugated Polymers. *Mater.* **2014**, *7*(3): 2273-2300; https://doi.org/10.3390/ma7032273.

[32] Sivalingam, G.; De, P.; Karthik, R.; Madras, G. Thermal Degradation Kinetics of Vinyl Polyperoxide Copolymers. *Polym. Degrad. Stab.* **2004**, *84*(1): 173-179; https://doi.org/10.1016/j.polymdegradstab.2003.10.008.

[33] Tuffi, R.; D'Abramo, S.; Cafiero, L.M.; Trinca, E.; Ciprioti, S.V. Thermal Behavior and Pyrolytic Degradation Kinetics of Polymeric Mixtures from Waste Packaging

Plastics. *eXPRESS Polym. Lett.* **2018**, *12*(1): 82-99; https://doi.org/10.3144/expresspolymlett.2018.7.
[34] Ries, A.; Canedo, E.L.; Souto, C.R.; Wellen, R.M. Non-Isothermal Cold Crystallization Kinetics of poly (3-Hydoxybutyrate) Filled with Zinc Oxide. *Thermochim. Acta* **2016**, *637*: 74-81; https://doi.org/10.1016/j.tca.2016.06.002.
[35] Alvarez, V.A.; Vázquez, A. Thermal Degradation of Cellulose Derivatives/Starch Blends and Sisal Fibre Biocomposites. *Polym. Degrad. Stab.* **2004**, *84*(1): 13-21; https://doi.org/10.1016/j.polymdegradstab.2003.09.003.
[36] Kongkaew, N.; Pruksakit, W.; Patumsawad, S. Thermogravimetric Kinetic Analysis of the Pyrolysis of Rice Straw. *Energy Procedia* **2015**, *79*: 663-670; https://doi.org/10.1016/j.egypro.2015.11.552.
[37] Pawar, A.; Panwar, N.L.; Jain, S.; Jain, N.K.; Gupta, T. Thermal Degradation of Coconut Husk Waste Biomass under non-Isothermal Condition. *Biomass Convers. Biorefin.* **2021**, *13*: 7613-7622; https://doi.org/10.1007/s13399-021-01657-w.
[38] Brachi, P.; Miccio, F.; Miccio, M.; Ruoppolo, G. Isoconversional Kinetic Analysis of Olive Pomace Decomposition under Torrefaction Operating Conditions. *Fuel Process. Technol.* **2015**, *130*: 147-154; https://doi.org/10.1016/j.fuproc.2014.09.043.
[39] Parr, R.G.; Yang, W. Density Functional Approach to the Frontier-Electron Theory of Chemical Reactivity. *J. Am. Chem. Soc.* **1984**, *106*(14): 4049-4050; https://doi.org/10.1021/ja00326a036.
[40] Alizadeh, M.; Bayat, Y. Influence of Functional Groups in Chemical Reactivity and Optoelectronic Properties of Novel Glycidyl Nitrate Copolymers (GNCOP): A DFT Study. *J. Mol. Model.* **2023**, *29*(3): paper 82; https://doi.org/10.1007/s00894-023-05480-0.
[41] Pakiari, A.H.; Eshghi, F. Geometric and Electronic Structures of Vanadium sub-nano Clusters, Vn (n = 2-5), and Their Adsorption Complexes with CO and O_2 Ligands: A DFT-NBO Study. *Phys. Chem. Res.* **2017**, *5*(3): 601-615; https://doi.org/10.22036/pcr.2017.80624.1364.
[42] Kruse, H.; Grimme, S. A Geometrical Correction for the inter- and intra-Molecular Basis Set Superposition Error in Hartree-Fock and Density Functional Theory Calculations for Large Systems. *J. Chem. Phys.* **2012**, *136*(15): paper 154101; https://doi.org/10.1063/1.3700154.
[43] Benjamin, I.; Gber, T.E.; Louis, H.; Ntui, T.N.; Oyo-Ita, E.I.; Unimuke, T.O.; Edim, M.M.; Adeyinka, A.S. Modelling of Aminothiophene-Carbonitrile Derivatives as Potential Drug Candidates for Hepatitis B and C. *Iran. J. Sci. Technol., Trans. A: Sci.* **2022**, *46*(5): 1399-1412; https://doi.org/10.1007/s40995-022-01355-w.
[44] Frisch, M.J.; Trucks, G.W.; Schlegel, H.B. *Gaussian 09. Revision D. 01 [CP]*. Gaussian. Inc., Wallingford/Pittsburgh, USA, **2013**, https://cir.nii.ac.jp/crid/1380567187536707208.
[45] Dong, Q.; Li, H.; Liu, X.; Huang, C. Thermal and Rheological Properties of PGN, PNIMMO and P (GN/NIMMO) Synthesized via Mesylate Precursors. *Propellants Explos. Pyrotech.* **2018**, *43*(3): 294-299; https://doi.org/10.1002/prep.201700201.
[46] Fodor, C.; Domján, A.; Iván, B. Unprecedented Scissor Effect of Macromolecular

cross-Linkers on the Glass Transition Temperature of poly (*N*-Vinylimidazole), Crystallinity Suppression of poly (Tetrahydrofuran) and Molecular Mobility by Solid State NMR in poly (*N*-Vinylimidazole)-l-poly (tetrahydrofuran) Conetworks. *Polym. Chem.* **2013**, *4*(13): 3714-3724; https://doi.org/10.1039/C3PY00299C.

[47] Satoh, K.; Kamigaito, M.; Sawamoto, M. Direct Living Cationic Polymerization of p-Hydroxystyrene with Boron Trifluoride Etherate in the Presence of Water. *Macromol.* **2000**, *33*(15): 5405-5410. https://doi.org/10.1021/ma991959d.

[48] Okada, M.; Kamachi, M.; Harada, A. Preparation and Characterization of Inclusion Complexes Between Methylated Cyclodextrins and poly (Tetrahydrofuran). *Macromol.* **1999**, *32*(21): 7202-7207; https://doi.org/10.1021/ma990806n.

[49] Dou, J.; Xu, M.; Tan, B.; Lu, X.; Mo, H.; Wang, B.; Liu, N. Research Progress of Nitrate Ester Binders. *FirePhysChem.* **2023**, *3*(1): 54-77, https://doi.org/10.1016/j.fpc.2022.09.003.

Received: July 2, 2023
Revised: February 27, 2024
First published online: February 29, 2024